

Hydraulic Fracture Geometry Inversion and Analysis of Influencing Factors Based on ABAQUS

Shukai Tang, Mingzhong Li* and Minhui Qi

School of petroleum engineering, China University of Petroleum, Qingdao, Shandong, China

*Corresponding author e-mail: limingzhong_upc@hotmail.com

Abstract. Based on the finite element software ABAQUS, the three-dimensional model of fluid-solid coupling hydrofracture expansion is established, and the hydraulic fractures are retrieved according to reservoir parameters. The effects on fracture propagation are analysed, including the injection pressure, the frac fluid viscosity, the maximum and minimum principal stress and Young's modulus of rock on fracture propagation. The results show that the maximum length and width of the fracture increase gradually with the increase of the injection pressure, but decrease with the increase of the elastic modulus. With the increase of the frac fluid viscosity, the maximum fracture length and width show two opposite trends. The maximum fracture length decreases with the increase of the viscosity, but the decreasing rate slows down gradually, showing the decreasing trend of the exponential function. However, with the increase of the viscosity, the maximum fracture width increases and the initiation pressure is not affected. When the minimum principal stress increases gradually, the maximum fracture length and width reduced gradually, and the initiation pressure also increases linearly, but the change of the maximum principal stress has no effect on the fracture initiation pressure.

1. Introduction

Hydraulic fracturing is an important technical countermeasure for reservoir development, and the fracture expansion form affects the effect of hydraulic fracturing development. Therefore, it is important to analyze the hydraulic fractures in accordance with the mechanical properties of the reservoirs and analyze the influencing factors of the fractures.

The hydrofracture expansion is a complex subject covering the fluid seepage, the rock deformation and fracture geometry coupling, which is affected by injection pressure, fluid viscosity, reservoir ground stress and Young's modulus of rock. With the development of fracturing optimization technology, the numerical simulation model of fracturing extension develops to the pseudo-3D model [1-5], until the current full three-dimensional model. Most of the mathematical solutions to these models use the finite difference, and assumes that the rock is linear elastic material rather than elastoplastic pore material [6], which is deviated from the actual situation. In recent years, finite element simulation technology has become an important technical to simulate the initiation and expansion of hydraulic fracturing. The ABAQUS can realize the solution of fluid-solid coupling and



analyze the factors that affect the geometry of hydrofracture [7-8]. Based on reservoir parameters, this paper uses ABAQUS to inverse the fracture growth patterns and analyzes the influencing factors.

2. Mathematical model

2.1. Equations of rock stress equilibrium and finite element

The rock is a porous medium consisting of the solid skeleton, the interconnected pores and the fluids (oil, gas and water) stored in the pores of the skeleton. There are two fluids stored in the pores of the porous medium, one is water and oil in liquid state, and the other is the gas. When the porous medium is partially saturated, both fluids are present at the same space, and when fully saturated, the pores are completely filled with liquid. When discussing the fluid-solid coupling of rock, the rock stress balance equation is considered first:

$$\sigma_{ij,j} + \hat{f}_i = 0 \quad (\text{in the region of } V) \quad (1)$$

Boundary condition:

$$\begin{cases} \sigma_{ij}n_j - t_i = 0 & (\text{on the force boundary of } S_\sigma) \\ u_{ij} = \bar{u}_i & (\text{on the displacement boundary of } S_u) \end{cases} \quad (2)$$

The weight function of the equilibrium equation in the region V is the weight function of velocity and the weight function of the force boundary condition, and we can obtain the integral equation which equivalent to the differential equation:

$$\int_V (\sigma_{ij,j} + f_i) \delta v_i dv - \int_{S_\sigma} (\sigma_{ij}n_j - t_i) \delta v_i dS \quad (3)$$

2.2. Continuity equation of fluid seepage

The time rate of change of fluid mass in the control volume V is:

$$\frac{d}{dt} \int_V \rho_w n_w dV = \int_V \frac{1}{J} \frac{d}{dt} (J \rho_w n_w) dV \quad (4)$$

The fluid mass entering the control body in a element time through the surface S is:

$$- \int_S \rho_w n_w n^T \cdot v_w dS \quad (5)$$

In the formula, v_w is the seepage velocity (velocity of the fluid relative to the solid skeleton), n^T is the outward normal direction of the surface S.

According to the law of conservation of mass, we can get:

$$\int_V \frac{1}{J} \frac{d}{dt} (J \rho_w n_w) dV = - \int_S \rho_w n_w n^T \cdot v_w dS \quad (6)$$

The flow of porous media is subject to Darcy's law, the formula is:

$$v_w = -\frac{1}{n_w g \rho_w} k \cdot \left(\frac{\partial p_w}{\partial x} - \rho_w g \right) \quad (7)$$

In the formula, k is the permeability coefficient vector, and g is the gravitational acceleration vector. The continuity condition of the fluid continuity equation is:

$$F = \begin{cases} -\frac{n^T}{n_w g \rho_w} k \cdot \left(\frac{\partial p_w}{\partial x} - \rho_w g \right) - \bar{q} = 0 & \left(\text{on } S_q \right) \\ p_w - \bar{p}_w = 0 & \left(\text{on } S_{p_w} \right) \end{cases} \quad (8)$$

In the formula, \bar{q} is the volume flow vector of fluid in element area which is given from the boundary of the fluid load, and \bar{p}_w is the pore pressure specified on the boundary condition of fluid pore pressure.

2.3. Fracture initiation of cohesive element

The maximum stress criterion assumes that when the stress under any direction reaches its critical stress, the cohesive element fractures up. The expression is:

$$\max \left\{ \frac{\langle t_n \rangle}{t_n^0}, \frac{t_s}{t_s^0}, \frac{t_t}{t_t^0} \right\} = 1 \quad (9)$$

In the formula, t_n^0 is the critical stress of the normal direction of the cohesive element, but also the tensile strength of the rock. t_s^0 and t_t^0 are the critical stresses of the first and the second tangential direction. The symbol $\langle \rangle$ indicates that the cohesive element can bear compressive stress or simultaneous deformation without damage.

2.4. Fluid flow properties of cohesive element

Tangential flow of fluid in cohesive element [9, 10]

$$qd = \frac{d^3}{12\mu} \nabla p \quad (10)$$

In the formula, q is the density vector of volumetric flow rate, and d is the fractured displacement of cohesive element. μ is the viscosity coefficient of frac fluid in cohesive element, and the ∇p is the pressure gradient of tangential flow fluid.

During the tangential flow, the fluid flows into the formation medium through the upper and lower surfaces of the cohesive element. The normal flow on the upper and lower surfaces of the cohesive element is calculated as follows:

$$\begin{cases} q_t = c_t (p_i - p_t) \\ q_b = c_b (p_i - p_b) \end{cases} \quad (11)$$

In the formula, q_t and q_b are the volumetric flow rate of the fluid flowing into the cohesive element through the upper and lower surfaces. c_t and c_b are the filtration coefficients of the upper and lower surfaces. p_t and p_t are the pore pressures of the upper and lower surfaces of the cohesive unit, and p_i is the fluid pressure in the cohesive unit.

3. Case Analysis

Table 1. Finite element model parameters of hydraulic fracturing simulation

model parameters	value
dimension of finite element model	300m×200m
maximum horizontal crustal stress	58MPa
minimum horizontal crustal stress	50MPa
viscosity of frac fluid	5mPa.s
frac fluid volume	4.5m ³ /min
reservoir thickness	18.2m
Young ' s modulus of horizontal direction	Ex=30GPa, Ey=20GPa
horizontal shear modulus	Gxy=Ex/2(1+PRxy)=2.69GPa; Gyx=Ey/2(1+PRyx)=2.38GPa;
horizontal Poisson's ratio	PRxy=0.293; PRyx=0.27
tensile strength of reservoir rock	6.2MPa
formation porosity	13.9%
formation reference permeability (mD)	20.3

The finite element model of the fractured formation is shown in figure 1.

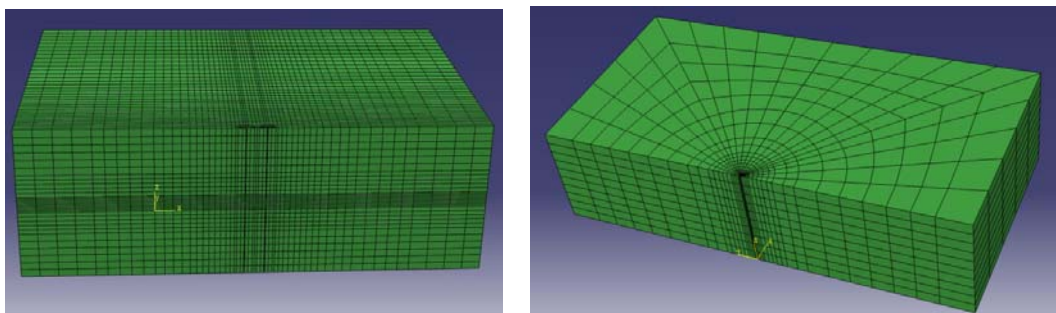


Figure 1. finite element model of the fractured formation

The formation model is analyzed by finite element method, and the pore pressure change of hydraulic fracturing is as shown in figure 2.

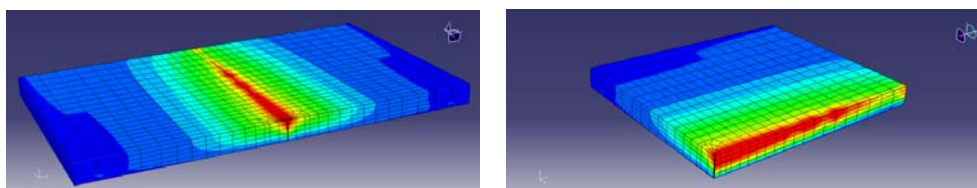


Figure 2. Distribution of formation pressure at fracture surface

As shown in figure 2, the distribution of fractures in the direction of fracture extension and vertical fracture is elliptical; the geometric parameters of fracture include half joint length of 178m, the slit width of 4.5mm and the seam height of 30m (figure 3).

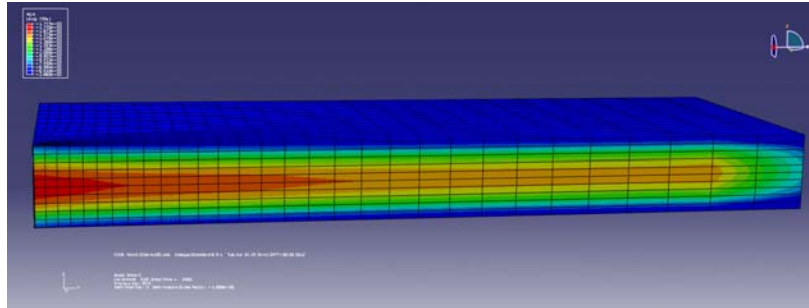


Figure 3. Distribution of formation pressure at fracture surface (sectional drawing)

As can be seen from the stratigraphic section, the half –length of the fracture is 162m, and the width is 5.4mm with the height of 24m.

After the frac fluid is injected according to the construction parameters, the pore pressure at the corresponding different formation depth is shown in figure 4.

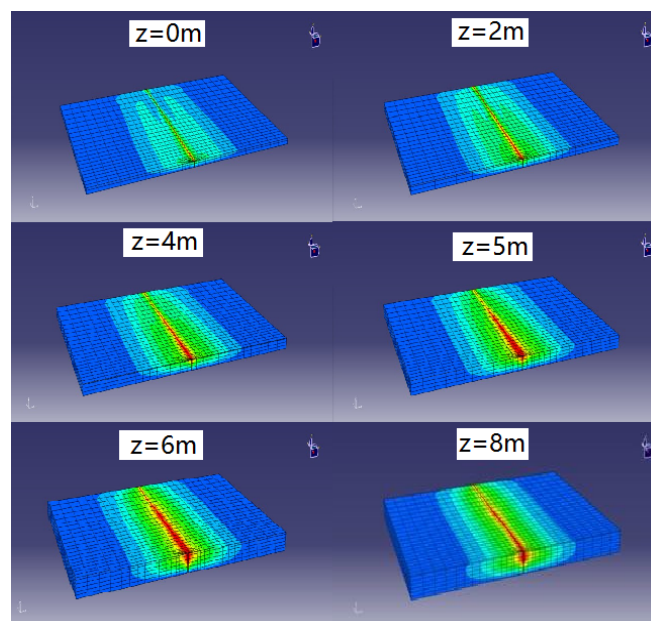


Figure 4. The pore pressure nearby the fractures at different depth

The frac fluid is injected at z of 5m, and the formation pressure at different depths shows elliptical distribution. The fluctuation range of the formation pressure is reduced far from the injection point. Figure 5 shows the variation of formation pore pressure at different distances from the wellbore.

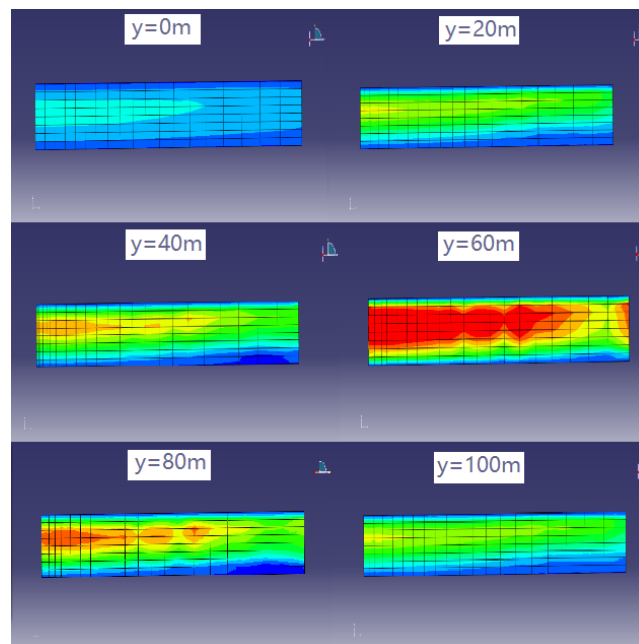


Figure 5. The formation pore pressure at different distances from the wellbore

The influence area of frac fluid injection reduces; the formation pressure is approximately elliptical in the vertical direction of Y (figure 6).

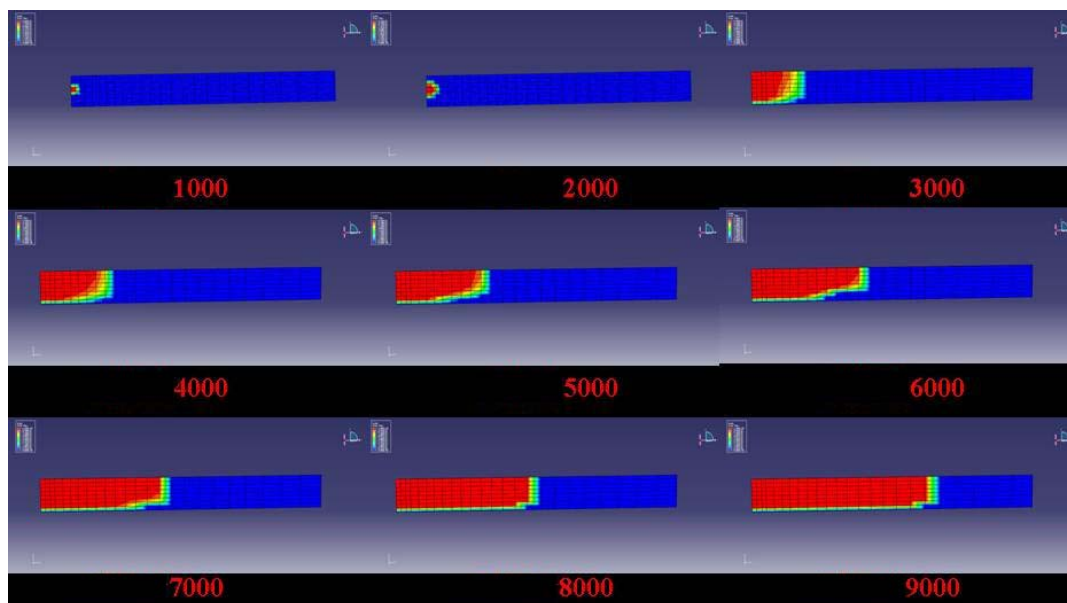


Figure 6. Variation of fracture with time during hydraulic fracturing -- geometry of fracture surface extension

Fracture width calculation results of Fan162- inclined 15 well (fracture width enlarged 500 times) as shown in figure 7.

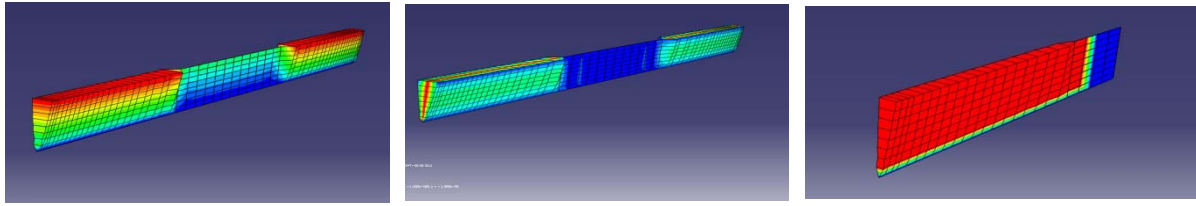


Figure 7. Calculation results of fracturing fracture displacement (fracture width enlarged 500 times)

The calculation results show that the hydraulic fracture width is 4.5mm with the height of 30m; the fracture is approximately elliptical along the width direction (figure 8).

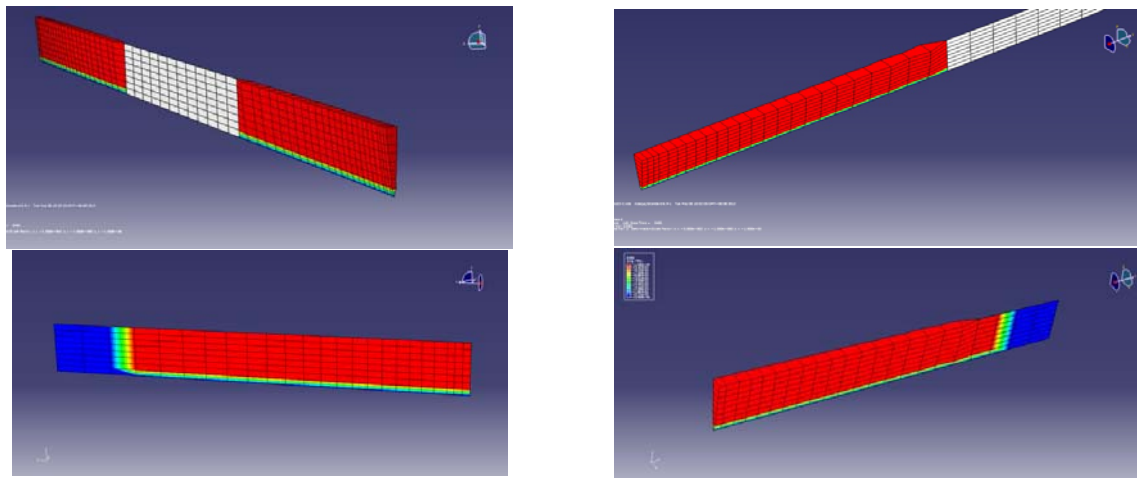


Figure 8. Damage factor distribution and fracture geometry of Cohesive unit (The fracture width is magnified 50 times)

For the COHESIVE unit, SDEG is a standard to measure its damage. When SDEG equals 1, the COHESIVE unit fails and the distribution of the COHESIVE unit is the geometry of the fracture.

4. Analysis of influencing factors of hydraulic fracture geometry

(1) Injection pressure

The effect of the injection pressure on the fracture geometry is shown in figure 9 and 10.

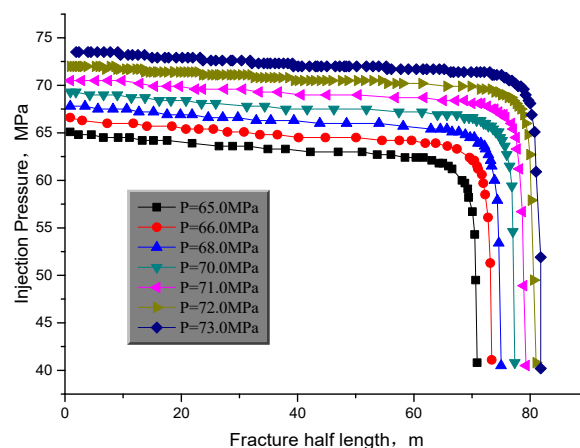


Figure 9. Distribution of frac fluid pressure on fractured surface under different injection pressure

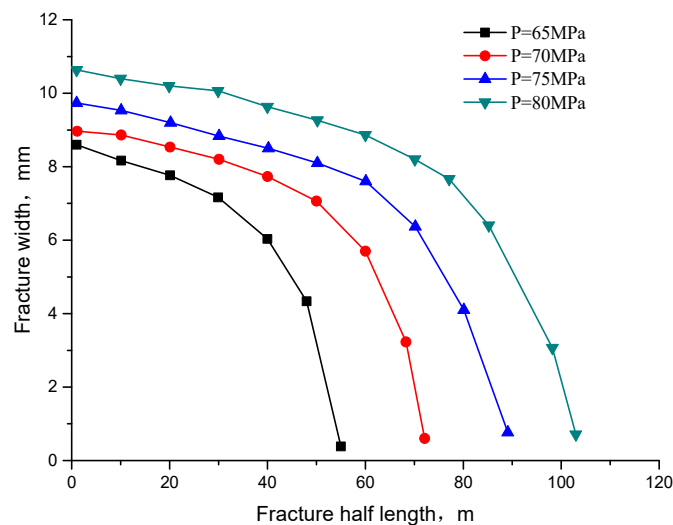


Figure 10. Fracture geometry under different injection pressures

As we can see from the figure, when the injection pressure increase, the tensile stress of frac fluid acting on the fracture surface increases and fractures gradually widened. Therefore, as the injection pressure increases, the hydraulic pressure attenuation in the fracture surface gradually slow down and the hydraulic pressure drop curves tend to be smooth.

Under different injection pressures, the shape of the fractures is approximately elliptical. As the injection pressure increases, the maximum length width of the fractures is gradually increased.

(2) The elasticity modulus of reservoir (Figure 11 and 12)

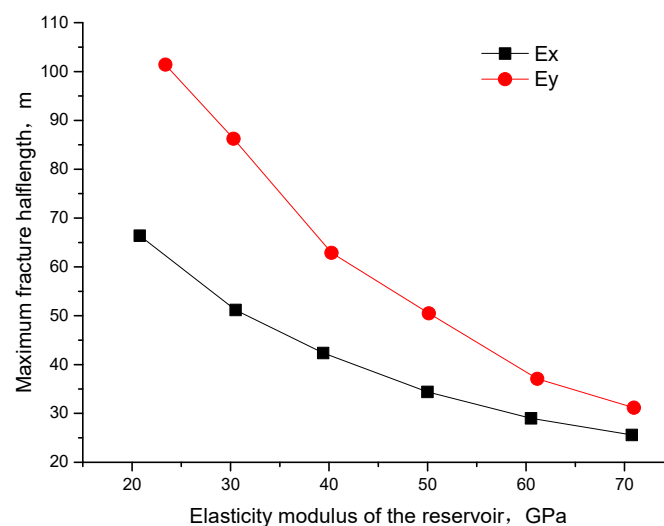


Figure 11. Relationship between the maximum fracture length and the elasticity modulus of reservoir

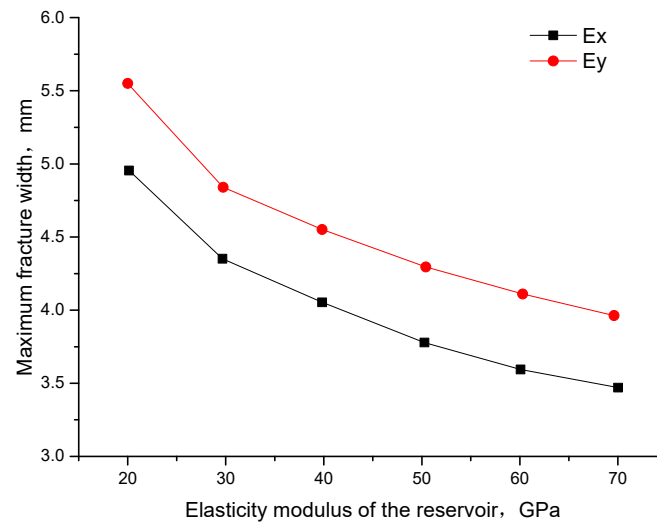


Figure 12. Relationship between the maximum fracture width and the elasticity modulus of reservoir

The elasticity modulus of reservoir rocks has a significant influence on the development of fracture geometry, and the maximum length and width of fracture decrease with the increase of elasticity modulus.

(3) Viscosity of fracturing fluid

The influence of the fracturing fluid viscosity on the fracture geometry is shown in figures 13-16.

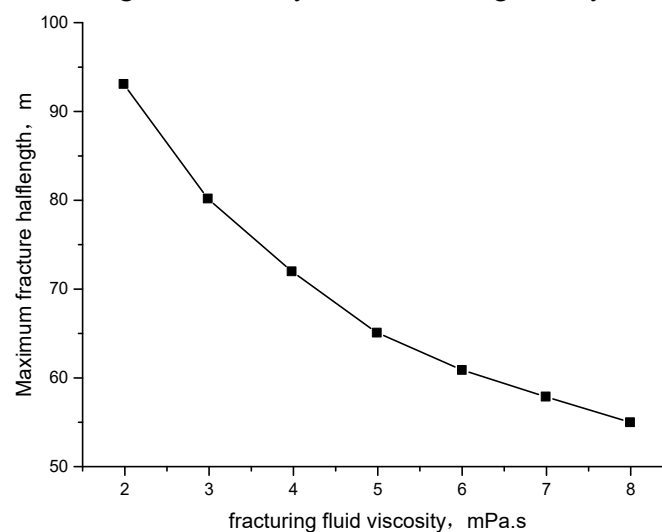


Figure 13. Relationship between the maximum fracture length and viscosity of fracturing fluid

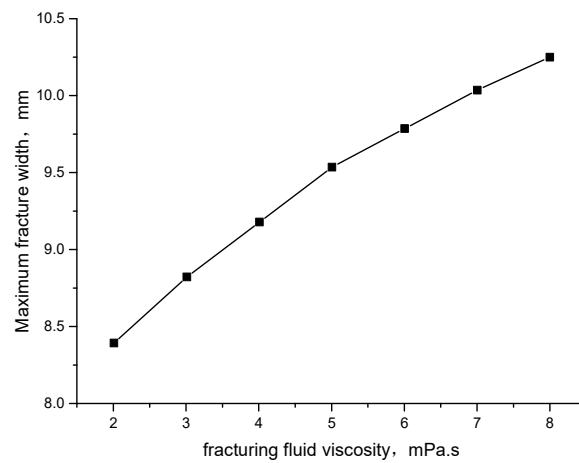


Figure 14. Relationship between the maximum fracture width and viscosity of fracturing fluid

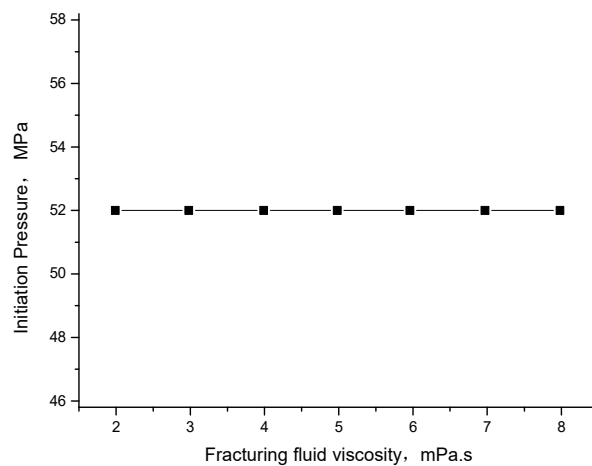


Figure 15. Relationship between initiation pressure and viscosity of fracturing fluid

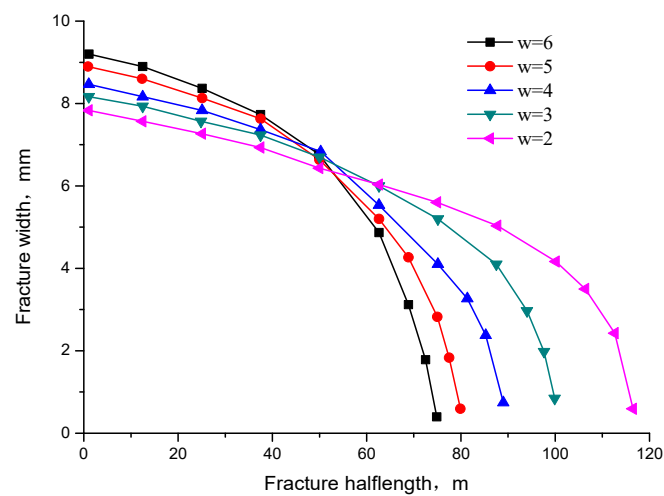


Figure 16. Fracture geoetry under different fracturing fluid viscosities

It can be seen that with the increase of fracturing fluid viscosities, the maximum fracture length and width showed two opposite trends. The maximum fracture length decreases, but the decreasing rate gradually slowed down, showing an overall decreasing trend of exponential function. By contrast, the maximum fracture width increases gradually with the increase of fracturing fluid viscosities.

It can be seen from the diagram that the initiation pressure is not affected by the fracturing fluid viscosity; when the viscosity of the fracturing fluid increases, the fracture becomes wide and short; when the viscosity of the fracturing fluid decreases, the fracture becomes narrow and long, which is consistent with the analysis.

The maximum and minimum principal stress of reservoir is shown in figures 17-19.

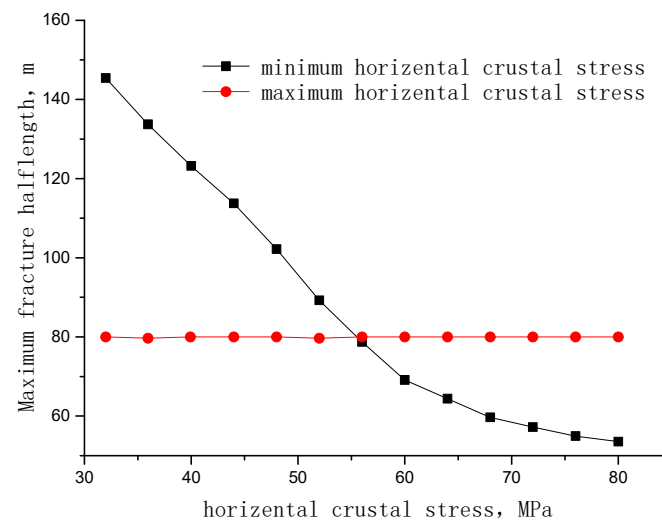


Figure 17. Relationship between the maximum fracture length and

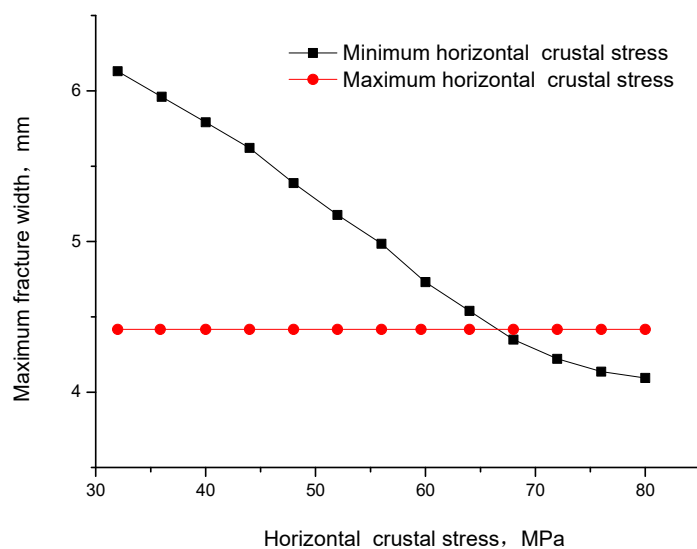


Figure 18. Relationship between the maximum fracture width and horizontal crustal stress

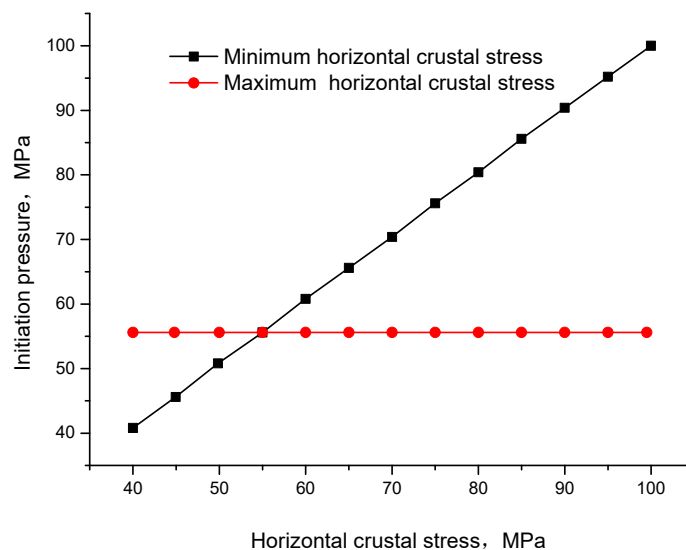


Figure 19. Relationship between the initiation pressure and horizontal crustal stress

It can be seen that when the minimum principal stress increases, the maximum fracture length and the maximum width decreases, and the fracturing pressure also increases linearly; the change of maximum principal stress has no effect on initiation pressure.

5. Conclusion

The mathematical model of fracture expansion is established by fluid-solid coupling finite element method. According to the formation parameters of a block, the fracture geometry is inversed, and the factors affecting the fracture geometry are analysed. The following conclusions are obtained:

(1) Therefore, with the increase of injection pressure, the attenuation of hydraulic pressure in the fracture surface gradually slows down, and the hydraulic pressure drop curve tends to be smooth; under different injection pressures, the fracture geometry is approximately elliptical. With the increase of injection pressure, the maximum length and the maximum width of fractures gradually increase.

(2) The elastic modulus of reservoir rocks has a significant influence on the development of fracture geometry, and the maximum length and maximum width of fracture decrease with the increase of elastic modulus.

(3) With the increase of fracturing fluid viscosities, the maximum fracture length and width showed two opposite trends. The maximum fracture length decreases, but the decreasing rate gradually slowed down, showing an overall decreasing trend of exponential function. By contrast, the maximum fracture width increases gradually with the increase of fracturing fluid viscosities. The initiation pressure is not affected by the fracturing fluid viscosity; when the viscosity of the fracturing fluid increases, the fracture becomes wide and short; when the viscosity of the fracturing fluid decreases, the fracture becomes narrow and long

(4) When the minimum principal stress increases, the maximum fracture length and the maximum width decreases, and the fracturing pressure also increases linearly; the change of maximum principal stress has no effect on initiation pressure.

References

- [1] Jinzhou Zhao, Shuquan Ren. Numerical calculation model and method of fracture size considering temperature influence [J]. Journal of Petroleum Science, 1987, 8(1): 71-82.
- [2] Ping Zhang. Numerical simulation of two dimensional fracture propagation in hydraulic

- fracturing [J]. Oil Drilling and Production Technology, 1997, 19(3): 53-59.
- [3] YEW C H, MA M J, HILL A D. A study of fluid leakoff in hydraulic fracture propagation [R]. SPE 64786, 2000.
- [4] VAN Dam D B, PAPANASTASIOU P. Impact of rock plasticity on hydraulic; fracture propagation and closure [R]. SPE 63172, 2000.
- [5] LEE, JANTZ E L. A Three-dimensional hydraulic propagation theory coupled with two-dimensional proppant transport [R]. SPE 19770, 1989.
- [6] Shicheng Zhang, Jin Zhang. Theory and application of fracturing development [M]. Beijing: Petroleum Industry Press, 2003.
- [7] Hongxun Zhang, Shicheng Zhang. Numerical calculation method for hydraulic fracturing design [M]. Beijing: Petroleum Industry Press, 1998.
- [8] Han Wang, He Liu, Jin Zhang. Numerical simulation study on high seam control parameters of hydraulic fractures [J]. Journal of University of Science and Technology of China, 2011, 41 (9): 820-825.
- [9] Fangjun Biao. Numerical simulation of horizontal fracture propagation in hydraulic fracturing [D]. Beijing: University of Science and Technology China, 2011.
- [10] Yiping Shi, Yurong Zhou. Detailed analysis of ABAQUS finite element analysis [M]. Beijing: Machinery Industry Press, 2006.